

An Electricity Market with Reactive Power Trading: Incorporating Dynamic Operating Envelopes

Zeinab Salehi, Elizabeth L. Ratnam, Yijun Chen, Ian R. Petersen, Guodong Shi, and Duncan S. Callaway

Abstract—Electricity market design that accounts for grid constraints such as voltage and thermal limits at the distribution level can increase opportunities for the grid integration of Distributed Energy Resources (DERs). In this paper, we consider rooftop solar backed by battery storage connected to a distribution grid. We design an electricity market to support customers sharing rooftop generation in excess of their energy demand, where customers earn a profit through peer-to-peer (P2P) energy trading. Our proposed electricity market also incorporates P2P reactive power trading to improve the voltage profile across a distribution feeder. We formulate the electricity market as an optimization-based problem, where voltage and thermal limits across a feeder are managed through the assignment of customer-specific dynamic operating envelopes (DOEs). The electricity market equilibrium is referred to as a competitive equilibrium, which is equivalent to a Nash equilibrium in a standard game. Our proposed market design is benchmarked using the IEEE 13-node test feeder.

I. INTRODUCTION

Power systems are transitioning from centralized fossil fuel-based generation to renewable-based operations — with a more geographically distributed energy mix. An element of the energy transition is the recent rapid uptake of distributed energy resources (DERs), including rooftop solar backed by battery storage systems, and electric vehicles (EVs). As electricity end-users become equipped with DERs, providing the means to both consume and generate electricity (i.e., an energy prosumer), new opportunities arise to participate in electricity markets [1]. To efficiently operate distribution networks with growing populations of prosumers, new market mechanisms that support both energy trading and voltage regulation at the distribution-level are required [2].

An energy trading market operator in a competitive market determines the price for electricity, and sets the price according to the law of supply and demand [3], [4]. In a competitive energy market, prosumers are considered small relative to the market size, and accordingly, individual decisions of

prosumers do not influence the price [3]. Once the market operator sets the electricity price, each prosumer seeks to maximize their payoff [5], a combination of the cost of electricity consumption and income from electricity trading. The market reaches a *competitive equilibrium* when no participant has an incentive to change their decision, and total supply matches total demand [6]–[8].

To efficiently operate an electric grid, physics-based constraints, including voltage and thermal limits, must also be considered in the design of a new market mechanism. Distribution Network Service Providers (DNSPs) typically impose static limits on customer imports and exports to ensure feeder-level voltage and thermal limits remain within permissible operating envelopes. However, static import and export limits are conservative, as they do not reflect time-varying grid conditions [9]. Accordingly, DNSPs are increasingly adopting flexible grid connection agreements with prosumers, supporting operations with Dynamic Operating Envelopes (DOEs) [10]. Specifically, a DOE is computed by a DNSP and is communicated to a prosumer — providing a range of permissible active and reactive power injections (or demand) at a given time [11].

Ancillary services are another element of an electricity market, improving the reliability and security of the electricity supply. Ancillary services have typically been provided by large, centralized generators. As we transition to renewable-based grid operations, ancillary services are increasingly being delivered by a wider range of participants, including prosumers with DERs [12]. Key ancillary services include frequency regulation [13], voltage support [2], and black-start capability [14]. That is, within DOE limits, prosumers can contribute to both energy trading and ancillary services. However, limited DOE implementation and insufficient incentives for prosumer-based reactive power regulation potentially reduce the efficiency of existing market operations [15], [16].

In this paper, we consider a radial distribution grid that connects customers with DERs, including rooftop solar, battery storage, and EVs. We assume prosumers regulate both real and reactive power via inverters to support energy trading and grid constraints such as voltage and thermal limits. We design a P2P energy market that enables both active power and reactive power trading between prosumers, achieving a balance in electricity supply and demand. Building on our prior work in [17], we ensure grid constraints are satisfied by localizing feeder-level grid constraints into prosumer level DOE constraints. To improve the overall utilization of the feeder, we design a market-mechanism

This work was supported by the Australian Research Council under grants DP190102158, DP190103615, LP210200473, and DP230101014.

Zeinab Salehi and Ian R. Petersen are with the School of Engineering, Australian National University, Canberra, ACT 2601, Australia (e-mail: zeinab.salehi@anu.edu.au; ian.petersen@anu.edu.au).

Elizabeth L. Ratnam is with the Department of Electrical and Computer Systems Engineering, Monash University, Melbourne, VIC 3168, Australia (e-mail: liz.ratnam@monash.edu).

Yijun Chen is with the Department of Electrical and Electronic Engineering, University of Melbourne, VIC 3052, Australia (e-mail: yijun.chen.1@unimelb.edu.au).

Guodong Shi is with the Australian Centre for Robotics, School of Aerospace, Mechanical and Mechatronic Engineering, The University of Sydney, NSW 2050, Australia (e-mail: guodong.shi@sydney.edu.au).

Duncan S. Callaway is with the Energy and Resources Group, University of California, Berkeley, CA 94720 USA (e-mail: dcal@berkeley.edu).

whereby prosumers trade any excess DOE capacity, which would otherwise remain unused. The main contributions of the paper are summarized in the following.

- We design an energy market with active and reactive power trading and DOE limit trading.
- We show that the market equilibrium is a competitive equilibrium and maximizes social welfare, defined as the sum of the utilities of all customers.
- We show that the proposed markets can be represented as a standard game, where prosumers are the players and a fictitious price-setting player determines the price, with the solution concept being a Nash equilibrium.

The rest of the paper is organized as follows. Section II introduces the prosumer dynamics and DOE constraints. Section III formulates the electricity market with reactive power trading to operate within feeder-level constraints. Section IV investigates the relation of the proposed market with the Nash equilibrium of a standard game. Section V presents numerical simulation results and Section VI concludes the paper.

II. PRELIMINARIES

We consider an electrical distribution feeder with a radial topology connecting N prosumers, each equipped with rooftop solar backed by battery storage. We consider the case where the electrical feeder operates in an island mode to support the blackstart capability of the bulk grid, i.e., all demand is met through local generation and P2P trading. We assume each prosumer has a home energy management system (EMS) that manages the rate of electricity consumption and energy trading according to the preferences of the prosumer. Within the EMS, the prosumer preferences are formulated into mathematical expressions termed the payoff, which is defined as the sum of the consumption utility (satisfaction level) and the income or expenditure from energy trading.

Each prosumer i , indexed in the set $\mathcal{N} = \{1, \dots, N\}$, has uncontrollable loads such as lighting, and controllable loads such as EVs and home battery storage systems. The net supply of each prosumer i is defined as the difference between the rooftop solar generation and uncontrollable load and is denoted by $a_i(t) \in \mathbb{R}$ (kW). Controllable loads are modeled by linear difference equations

$$\mathbf{x}_i(t+1) = \mathbf{A}_i \mathbf{x}_i(t) + \mathbf{B}_i \mathbf{u}_i(t), \quad t \in \mathcal{T}, \quad (1)$$

where $\mathbf{x}_i(t) \in \mathbb{R}^n$ is the dynamical state (e.g., the state of charge (SoC) of a battery), $\mathbf{x}_i(0) \in \mathbb{R}^n$ is the initial state (e.g., the initial SoC of a battery), and $\mathbf{u}_i(t) \in \mathbb{R}^m$ is the control input (e.g., the charge/discharge rate of a battery). Also, $\mathbf{A}_i \in \mathbb{R}^{n \times n}$ and $\mathbf{B}_i \in \mathbb{R}^{n \times m}$ are fixed matrices. States and control inputs are constrained by $\underline{\mathbf{x}}_i \leq \mathbf{x}_i(t) \leq \bar{\mathbf{x}}_i$ and $\underline{\mathbf{u}}_i \leq \mathbf{u}_i(t) \leq \bar{\mathbf{u}}_i$, where $\underline{\mathbf{x}}_i \in \mathbb{R}^n$ and $\underline{\mathbf{u}}_i \in \mathbb{R}^m$ denote lower bounds, and $\bar{\mathbf{x}}_i \in \mathbb{R}^n$ and $\bar{\mathbf{u}}_i \in \mathbb{R}^m$ denote upper bounds.

Prosumer preferences for managing controllable loads are expressed by utility functions $f_i(\mathbf{x}_i(t), \mathbf{u}_i(t)) : \mathbb{R}^n \times \mathbb{R}^m \mapsto \mathbb{R}$ that represent their satisfaction as a result of taking the control action $\mathbf{u}_i(t)$ and reaching the state $\mathbf{x}_i(t)$. For

example, if the SoC of the battery is close to 80% and the number of charge/discharge cycles are relatively low, then the prosumer potentially achieves a high level of satisfaction and a high $f_i(\cdot)$. Similarly, the terminal utility of a prosumer at the terminal time step T is denoted by $\phi_i(\mathbf{x}_i(T)) : \mathbb{R}^n \mapsto \mathbb{R}$, which depends on their satisfaction as a result of reaching the terminal state $\mathbf{x}_i(T)$. The average active power consumed or withdrawn as a result of the control action $\mathbf{u}_i(t)$ is denoted by $h_i(\mathbf{u}_i(t)) : \mathbb{R}^m \mapsto \mathbb{R}$ (kW). At each time step t , if an agent i has a supply shortage, i.e., $a_i(t) - h_i(\mathbf{u}_i(t)) < 0$, it can purchase the deficit from others; conversely, if it has a surplus, it can sell it to others through a trading decision variable $p_i(t) \in \mathbb{R}$ (kW) such that $p_i(t) \leq a_i(t) - h_i(\mathbf{u}_i(t))$ ¹. Active power injection is also constrained by inverter limits such that $\underline{p}_i \leq p_i(t) \leq \bar{p}_i$, where \underline{p}_i and \bar{p}_i denote the lower and upper bound inverter limits, respectively.

Behind-the-meter inverters with reactive power regulation capability can support voltage regulation grid services. The injected or absorbed reactive power by prosumer i is denoted by $q_i(t) \in \mathbb{R}$ (kVar) such that $\underline{q}_i \leq q_i(t) \leq \bar{q}_i$, where \underline{q}_i and \bar{q}_i represent the lower and upper bound inverter limits, respectively. All inverter-based voltage regulation across a distribution feeder must comply with physics-based grid limits.

A. Electric Grid Constraints

Denote $\mathbf{p}(t) = (p_1(t), \dots, p_N(t))^\top$ and $\mathbf{q}(t) = (q_1(t), \dots, q_N(t))^\top$ as the vectors of active and reactive power injections of all prosumers at time step $t \in \mathcal{T}$, respectively. We represent grid constraints in the separable form [11]

$$\mathbf{F}_t(\mathbf{p}(t), \mathbf{q}(t)) = \sum_{i=1}^N \mathbf{g}_{it}(p_i(t), q_i(t)) \leq \boldsymbol{\nu}(t), \quad t \in \mathcal{T}, \quad (2)$$

where $\mathbf{F}_t : \mathbb{R}^N \times \mathbb{R}^N \mapsto \mathbb{R}^M$ is an affine vector function, and M denotes the total number of grid constraints at time step $t \in \mathcal{T}$. Each function $\mathbf{g}_{it} : \mathbb{R} \times \mathbb{R} \mapsto \mathbb{R}^M$ is a local affine vector function associated with prosumer i capturing its contribution to the M global grid constraints at time step $t \in \mathcal{T}$. These functions are determined by grid characteristics such as line impedances and topology. The vector $\boldsymbol{\nu}(t) \in \mathbb{R}^M$ specifies the bounds on the grid constraints, derived by the physical and operational limits of the network. Two examples of constraints expressed in the form of (2) include voltage and thermal limits [11]. Details of voltage constraints are provided in [11], [17].

Enforcing the grid constraints in (2) requires assigning feasible operating limits to individual prosumers. Static export limits or fixed power factor settings are often too conservative, as they fail to reflect the time-varying network conditions. DOEs have emerged as a promising approach to address this challenge.

Definition 1 (as in [11]): A DOE is a nonempty, closed, and convex set $\Omega_{it} \subseteq \mathbb{R}^2$ in the $(p_i(t), q_i(t))$ space, that specifies an admissible region of active and reactive

¹This inequality applies to both surplus and deficit cases.

power injections for prosumer i at time t , that the grid can accommodate without violating operational and physical constraints.

Using the right-hand side decomposition (RHSD) method [18], the right-hand side of (2) can be expressed as $\boldsymbol{\nu}(t) = \sum_{i=1}^N \mathbf{w}_i(t)$, where $\mathbf{w}_i(t) \in \mathbb{R}^M$ represents the share of the M grid constraints assigned to prosumer i at time step t . Consequently, the grid constraints in (2) can be written as $\sum_{i=1}^N \mathbf{g}_{it}(p_i(t), q_i(t)) \leq \sum_{i=1}^N \mathbf{w}_i(t)$, which, when decomposed, yields the DOEs $\Omega_{it} = \{(p_i(t), q_i(t)) \in \mathbb{R}^2 : \mathbf{g}_{it}(p_i(t), q_i(t)) \leq \mathbf{w}_i(t)\}$ for each prosumer $i \in \mathcal{N}$ at time step $t \in \mathcal{T}$ [11]. There are infinitely many possible choices for the RHSD and DOEs. In this paper, we focus on an allocation that maximizes the potential active power injection to the grid, by solving

$$\begin{aligned} \max_{\mathbf{w}(t), \mathbf{p}(t), \mathbf{q}(t)} \quad & \sum_{i=1}^N \max\{0, p_i(t)\} - \epsilon O(\mathbf{w}(t)) \\ \text{s.t.} \quad & \mathbf{g}_{it}(p_i(t), q_i(t)) \leq \mathbf{w}_i(t) \\ & \sum_{i=1}^N \mathbf{w}_i(t) = \boldsymbol{\nu}(t), \quad i \in \mathcal{N}, \end{aligned} \quad (3)$$

where $\mathbf{w}(t) = (\mathbf{w}_1^\top(t), \dots, \mathbf{w}_N^\top(t))^\top$, and $\epsilon O(\mathbf{w}(t))$ is a regularization term with ϵ being a small positive number. The function $O(\mathbf{w}(t)) : \mathbb{R}^{NM} \mapsto \mathbb{R}$ captures the preferences of the network service provider in allocating DOE shares among prosumers. To promote fairness, we consider $O(\mathbf{w}(t)) = \|\mathbf{w}(t) - \bar{\mathbf{E}}\|$, where $\bar{\mathbf{E}} \in \mathbb{R}^{NM}$, $\bar{\mathbf{E}} = (\boldsymbol{\nu}^\top(t)/N, \dots, \boldsymbol{\nu}^\top(t)/N)^\top$ is the equality index. This choice of $O(\mathbf{w}(t))$ reflects that the network service provider tends to allocate close to equal DOEs to all prosumers [11]. Solving (3), the network service provider determines the optimal DOEs and communicates them to each prosumer i in the form of $\mathbf{g}_{it}(p_i(t), q_i(t)) \leq \mathbf{w}_i^*(t)$.

III. MARKET WITH REACTIVE POWER COMPENSATION

Prosumers connected to the islanded feeder need to share their resources to meet their demand. In this section, we formulate a P2P market with reactive power trading that facilitates this interaction. Let $\lambda(t) \in \mathbb{R}$ denote the price for active power trading and $\gamma(t) \in \mathbb{R}$ the price for reactive power trading at time step t . In our prior work [17], we showed that prosumers can also trade their excess DOE limits, i.e., $\mathbf{w}_i^*(t) - \mathbf{g}_{it}(p_i(t), q_i(t))$, through a decision variable $\mathbf{l}_i(t) \in \mathbb{R}^M$ at a price $\boldsymbol{\beta}(t) \in \mathbb{R}^M$, subject to $\mathbf{l}_i(t) \leq \mathbf{w}_i^*(t) - \mathbf{g}_{it}(p_i(t), q_i(t))$, which mitigates the conservatism introduced by decomposing global grid constraints into local DOEs. In the following, we design a market that allows real and reactive power trading as well as DOE limit trading.

Obtaining DOE limits $\mathbf{w}_i^*(t)$ from (3), the coordinator determines equilibrium prices for active power trading $\lambda^*(t)$, reactive power trading $\gamma^*(t)$, and DOE limit trading $\boldsymbol{\beta}^*(t)$ that clear the market for $t \in \mathcal{T}$, and broadcasts them to participants. Upon receiving the equilibrium prices, prosumers engage in a P2P competitive market to maximize their payoff, defined as the sum of their utility $f_i(\mathbf{x}_i(t), \mathbf{u}_i(t))$, terminal

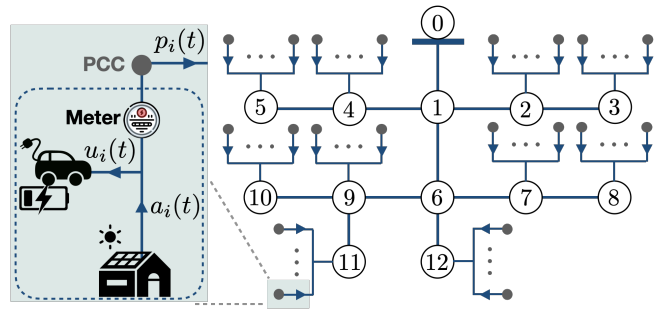


Fig. 1: Modified IEEE 13-node test feeder. Left: A prosumer i is zoomed in.

utility $\phi_i(\mathbf{x}_i(T))$, and the income $\lambda(t)p_i(t) + \gamma(t)q_i(t) + \boldsymbol{\beta}(t) \cdot \mathbf{l}_i(t)$ from transactions.

The market reaches an equilibrium when no participant has an incentive to change their decision and total supply equals total demand, i.e., the market clears. This equilibrium is called a *competitive equilibrium*, defined as follows. Let $\mathbf{p}_i = (p_i(0), \dots, p_i(T-1))^\top$, $\mathbf{q}_i = (q_i(0), \dots, q_i(T-1))^\top$, $\mathbf{L}_i = (\mathbf{l}_i^\top(0), \dots, \mathbf{l}_i^\top(T-1))^\top$, and $\mathbf{U}_i = (\mathbf{u}_i^\top(0), \dots, \mathbf{u}_i^\top(T-1))^\top$ denote, respectively, the vectors of active power injections, reactive power injections, traded DOE limits, and control inputs of prosumer i over the entire time horizon.

Definition 2: Optimal decisions $(\mathbf{u}_1^*(t), p_1^*(t), q_1^*(t), \mathbf{l}_1^*(t), \dots, \mathbf{u}_N^*(t), p_N^*(t), q_N^*(t), \mathbf{l}_N^*(t))$, along with optimal prices $\lambda^*(t)$, $\gamma^*(t)$, and $\boldsymbol{\beta}^*(t)$ for all $t \in \mathcal{T}$, form a *competitive equilibrium* if the following statements hold.

- (i) Given $\lambda^*(t)$, $\gamma^*(t)$, $\boldsymbol{\beta}^*(t)$, and $\mathbf{w}_i^*(t)$, each prosumer $i \in \mathcal{N}$ maximizes their payoff at $(\mathbf{u}_i^*(t), p_i^*(t), q_i^*(t), \mathbf{l}_i^*(t))$ for $t \in \mathcal{T}$ as a solution to

$$\begin{aligned} \max_{\mathbf{u}_i, \mathbf{p}_i, \mathbf{q}_i, \mathbf{L}_i} \quad & \sum_{t=0}^{T-1} \left(f_i(\mathbf{x}_i(t), \mathbf{u}_i(t)) + \lambda^*(t)p_i(t) \right. \\ & \left. + \gamma^*(t)q_i(t) + \boldsymbol{\beta}^*(t) \cdot \mathbf{l}_i(t) \right) + \phi_i(\mathbf{x}_i(T)) \\ \text{s.t.} \quad & \mathbf{x}_i(t+1) = \mathbf{A}_i \mathbf{x}_i(t) + \mathbf{B}_i \mathbf{u}_i(t), \\ & p_i(t) \leq a_i(t) - h_i(\mathbf{u}_i(t)), \\ & \mathbf{l}_i(t) \leq \mathbf{w}_i^*(t) - \mathbf{g}_{it}(p_i(t), q_i(t)), \\ & \underline{\mathbf{x}}_i \leq \mathbf{x}_i(t) \leq \bar{\mathbf{x}}_i, \quad \underline{\mathbf{u}}_i \leq \mathbf{u}_i(t) \leq \bar{\mathbf{u}}_i, \\ & \underline{p}_i \leq p_i(t) \leq \bar{p}_i, \quad \underline{q}_i \leq q_i(t) \leq \bar{q}_i, \quad t \in \mathcal{T}. \end{aligned} \quad (4)$$

- (ii) All traded power and all traded DOE limits are balanced at each time step; that is,

$$\sum_{i=1}^N p_i^*(t) = 0, \quad \sum_{i=1}^N q_i^*(t) = 0, \quad \sum_{i=1}^N \mathbf{l}_i^*(t) = 0, \quad t \in \mathcal{T}. \quad (5)$$

From microeconomics theory, a market outcome is Pareto efficient if there is no waste in the allocation of resources. Mathematically, a market outcome $(\mathbf{u}_1^*(t), p_1^*(t), q_1^*(t), \mathbf{l}_1^*(t), \dots, \mathbf{u}_N^*(t), p_N^*(t), q_N^*(t), \mathbf{l}_N^*(t))$ for all $t \in \mathcal{T}$ is efficient if it maximizes the social welfare of the society, defined as the sum of all

participant utilities $f_i(\cdot)$ and $\phi_i(\cdot)$, subject to local and global constraints. Such an operating point $(\mathbf{u}_1^*(t), p_1^*(t), q_1^*(t), \mathbf{l}_1^*, \dots, \mathbf{u}_N^*(t), p_N^*(t), q_N^*(t), \mathbf{l}_N^*)$ for all $t \in \mathcal{T}$ is referred to as a *social welfare maximization solution* and solves

$$\begin{aligned} & \max_{\mathbf{U}, \mathbf{P}, \mathbf{Q}, \mathbf{L}} \sum_{i=1}^N \left(\sum_{t=0}^{T-1} f_i(\mathbf{x}_i(t), \mathbf{u}_i(t)) + \phi_i(\mathbf{x}_i(T)) \right) \\ \text{s.t. } & \mathbf{x}_i(t+1) = \mathbf{A}_i \mathbf{x}_i(t) + \mathbf{B}_i \mathbf{u}_i(t), \\ & p_i(t) \leq a_i(t) - h_i(\mathbf{u}_i(t)), \\ & \mathbf{l}_i(t) \leq \mathbf{w}_i^*(t) - \mathbf{g}_{it}(p_i(t), q_i(t)), \\ & \sum_{i=1}^N p_i(t) = 0, \quad \sum_{i=1}^N q_i(t) = 0, \quad \sum_{i=1}^N \mathbf{l}_i(t) = 0, \\ & \underline{\mathbf{x}}_i \leq \mathbf{x}_i(t) \leq \bar{\mathbf{x}}_i, \quad \underline{\mathbf{u}}_i \leq \mathbf{u}_i(t) \leq \bar{\mathbf{u}}_i, \\ & \underline{p}_i \leq p_i(t) \leq \bar{p}_i, \quad \underline{q}_i \leq q_i(t) \leq \bar{q}_i, \quad i \in \mathcal{N}, \quad t \in \mathcal{T}, \end{aligned} \quad (6)$$

where $\mathbf{P} = (\mathbf{p}_1^\top, \dots, \mathbf{p}_N^\top)^\top$, $\mathbf{Q} = (\mathbf{q}_1^\top, \dots, \mathbf{q}_N^\top)^\top$, $\mathbf{L} = (\mathbf{l}_1^\top, \dots, \mathbf{l}_N^\top)^\top$, and $\mathbf{U} = (\mathbf{U}_1^\top, \dots, \mathbf{U}_N^\top)^\top$ denote, respectively, the vectors of all active power injection, reactive power injection, traded DOE limits, and control inputs of all prosumers over the entire time horizon.

In the following theorem, we show that the market outcome in Definition 2 is Pareto efficient, maximizing (6).

Theorem 1: Suppose $f_i(\cdot)$, $\phi_i(\cdot)$, and $-h_i(\cdot)$ are concave functions for $i \in \mathcal{N}$, and Slater's condition holds for (4) and (6). Given feasible initial conditions $\mathbf{x}_i(0)$ for $i \in \mathcal{N}$, the following statements hold.

- A competitive equilibrium in Definition 2 is equivalent to a social welfare maximization solution to (6).
- Let $-\alpha^*(t)$, $-\vartheta^*(t)$, and $-\delta^*(t)$ be optimal dual variables corresponding to the balancing equality constraints $\sum_{i=1}^N p_i(t) = 0$, $\sum_{i=1}^N q_i(t) = 0$, and $\sum_{i=1}^N \mathbf{l}_i(t) = 0$ in (6), respectively, for $t \in \mathcal{T}$. Then, equilibrium prices can be obtained as $\lambda^*(t) = \alpha^*(t)$, $\gamma^*(t) = \vartheta^*(t)$, and $\beta^*(t) = \delta^*(t)$ for $t \in \mathcal{T}$.

Proof: See Appendix I. \blacksquare

A procedure for implementing the proposed P2P market in Definition 2 is described in Algorithm 1.

Algorithm 1 Implementation of the P2P Market

- 1:** DNSP determines DOEs by solving (3) and sends $\mathbf{w}_i^*(t)$ to each prosumer i .
 - 2:** DNSP computes market prices $\lambda^*(t)$, $\gamma^*(t)$, and $\beta^*(t)$ as the optimal dual variables corresponding to the balancing constraints in (6), and broadcasts them to prosumers.
 - 3:** Prosumers form a P2P market and trade resources to maximize their payoff in (4).
-

Remark 1: Although Algorithm 1 employs a centralized approach in Step 2 to determine market prices, decentralized alternatives such as the Alternating Direction Method of Multipliers (ADMM) or dual decomposition can also be applied, as in [19], [20]. In these methods, prosumers obtain resource prices in a decentralized manner, either with or

without the supervision of a central coordinator. Following a procedure similar to [20], a fully decentralized and iterative scheme based on the dual decomposition method can be established for the P2P market proposed in Definition 2. In a fully decentralized P2P framework, prosumers independently determine resource prices, and all information exchange occurs among neighboring participants without central coordination. Such approaches preserve participant privacy.

IV. NASH EQUILIBRIUM

In this section, we examine the connection between the proposed market and a standard game. We show that the market outcome in Definition 2 can be implemented as a Nash equilibrium of a standard game with $N + 1$ players.

- The first player is an aggregator who takes the role of a price player and regulates the price such that the market clears. Given $p_i(t)$, $q_i(t)$, and $\mathbf{l}_i(t)$ for $i \in \mathcal{N}$ and $t \in \mathcal{T}$, the price player obtains uniform prices $\lambda(t)$, $\gamma(t)$, and $\beta(t)$ as a solution to

$$\max_{\lambda, \gamma, \beta} \sum_{i=1}^N \sum_{t=0}^{T-1} \left(-\lambda(t)p_i(t) - \gamma(t)q_i(t) - \beta(t) \cdot \mathbf{l}_i(t) \right), \quad (7)$$

where $\boldsymbol{\lambda} = (\lambda(0), \dots, \lambda(T-1))^\top$, $\boldsymbol{\gamma} = (\gamma(0), \dots, \gamma(T-1))^\top$, and $\boldsymbol{\beta} = (\beta^\top(0), \dots, \beta^\top(T-1))^\top$ are the vectors of all active power, reactive power, and DOE limit prices over the entire time horizon, respectively.

- The last N players are prosumers who maximize their payoff subject to the local constraints. Given prices $\lambda(t)$, $\gamma(t)$, and $\beta(t)$ for $t \in \mathcal{T}$, each prosumer $i \in \mathcal{N}$ obtains $(\mathbf{U}_i, \mathbf{p}_i, \mathbf{q}_i, \mathbf{L}_i)$ as a solution to

$$\begin{aligned} & \max_{\mathbf{U}_i, \mathbf{p}_i, \mathbf{q}_i, \mathbf{L}_i} \sum_{t=0}^{T-1} f_i(\mathbf{x}_i(t), \mathbf{u}_i(t)) + \phi_i(\mathbf{x}_i(T)) \\ & + \sum_{t=0}^{T-1} \left(\lambda(t)p_i(t) + \gamma(t)q_i(t) + \beta(t) \cdot \mathbf{l}_i(t) \right) \\ \text{s.t. } & \mathbf{x}_i(t+1) = \mathbf{A}_i \mathbf{x}_i(t) + \mathbf{B}_i \mathbf{u}_i(t), \\ & p_i(t) \leq a_i(t) - h_i(\mathbf{u}_i(t)), \\ & \mathbf{l}_i(t) \leq \mathbf{w}_i^*(t) - \mathbf{g}_{it}(p_i(t), q_i(t)), \\ & \underline{\mathbf{x}}_i \leq \mathbf{x}_i(t) \leq \bar{\mathbf{x}}_i, \quad \underline{\mathbf{u}}_i \leq \mathbf{u}_i(t) \leq \bar{\mathbf{u}}_i, \\ & \underline{p}_i \leq p_i(t) \leq \bar{p}_i, \quad \underline{q}_i \leq q_i(t) \leq \bar{q}_i, \quad t \in \mathcal{T}. \end{aligned} \quad (8)$$

The standard game in (7)–(8) stems from the generalized game introduced in [4], where the objective function of the price player indicates the “law of supply and demand”.

Theorem 2: Let $(\mathbf{U}^*, \mathbf{P}^*, \mathbf{Q}^*, \mathbf{L}^*)$, along with $\lambda^*(t)$, $\gamma^*(t)$, $\beta^*(t)$ for $t \in \mathcal{T}$, be a Nash equilibrium for the standard game in (7)–(8). Then $(\mathbf{U}^*, \mathbf{P}^*, \mathbf{Q}^*, \mathbf{L}^*)$, along with $\lambda^*(t)$, $\gamma^*(t)$, $\beta^*(t)$ for $t \in \mathcal{T}$, is equivalent to a competitive equilibrium as defined in Definition 2.

Proof: A Nash equilibrium is obtained when $\sum_{i=1}^N p_i^*(t) = 0$, $\sum_{i=1}^N q_i^*(t) = 0$, and $\sum_{i=1}^N \mathbf{l}_i^*(t) = 0$ for $t \in \mathcal{T}$, and therefore, the objective of the first player in (7) has a finite solution. This is equivalent to the second

condition in Definition 2. Additionally, a Nash equilibrium is obtained when the objective of the last N players in (8) is maximized, which corresponds to the first condition in Definition 2. Consequently, it is straightforward to show that $(\mathbf{U}^*, \mathbf{P}^*, \mathbf{Q}^*, \mathbf{L}^*)$, along with $\lambda^*(t), \gamma^*(t), \beta^*(t)$ for $t \in \mathcal{T}$, satisfies all the conditions in Definition 2. Furthermore, all competitive equilibria in Definition 2 serve as a Nash equilibrium for the game defined by (7)–(8). ■

V. NUMERICAL SIMULATIONS

In this section, we benchmark the proposed market with reactive power trading against one without reactive power participation. For simplicity, we consider voltage constraints in the electric grid; extensions to include thermal constraints are straightforward. We use a modified single-phase representation of the IEEE 13-node test feeder, as shown in Fig. 1, where the transformer between nodes 2 and 3, the switch between nodes 6 and 7, and all capacitor banks are omitted [21]. All simulations are conducted in Python 3.8 using CVXPY on a MacBook Pro with an Apple M1 chip and 16 GB of memory.

A. Simulation Setup

Apart from the feeder node, node 1, and node 6, each node is connected to 30 distribution aggregators. Each aggregator manages 11 residential prosumers, each equipped with a grid-connected EV and a home battery storage system. The net power supply of each prosumer—defined as rooftop solar generation minus uncontrollable demand—is derived from metering data provided by Ausgrid [22], an Australian electricity distribution network provider. This dataset, originally collected in 2012, is scaled by a factor of 2 to reflect increased solar generation and electrification levels. EV models are from a diverse set documented in [23], with battery capacities ranging from 0 to 75 (kWh). The corresponding home battery storage systems are assumed to have similar capacity characteristics. The charge/discharge efficiencies of EVs and home battery storage systems are assumed to be $\eta = 0.9$. The system is simulated over a 24-hour (h) time horizon starting at midnight, with a sampling time of $\Delta = 0.5$ (h).

The aggregated behavior of each aggregator i , incorporating both EVs and home battery storage systems of the associated 11 prosumers, is modeled using the linear difference equation $\mathbf{x}_i(t+1) = \mathbf{x}_i(t) + \eta \mathbf{u}_i(t) \Delta$, where $\mathbf{x}_i(t) \in \mathbb{R}^2$ denotes the SoC vector (kWh) of the aggregated EVs and residential battery storage systems, and $\mathbf{u}_i(t) \in \mathbb{R}^2$ represents the corresponding charge/discharge rate vector (kW) at each time step t . In both vectors, the first element corresponds to the aggregated EVs, and the second to the aggregated home battery storage systems. The initial SoC of each battery is assumed to follow a uniform distribution over the interval $[0.2, 0.5]$ of its respective capacity. Home battery storage systems remain grid-connected at all times, whereas EV arrival and departure times are drawn from survey data collected by the Victorian Department of Transport in Australia [24]. Prosumers are assumed to use level-2

chargers with a maximum charge rate of 6.6 (kW) [21], and a corresponding maximum discharge rate of -6.6 (kW). To preserve battery health, the SoC of both EVs and home battery storage systems is constrained to remain between 20% and 85% of their respective capacities. Accordingly, the aggregated SoC and charging/discharging rates for each aggregator i are bounded by $0.2\mathbf{C}_i \leq \mathbf{x}_i(t) \leq 0.85\mathbf{C}_i$ and $-6.61 \leq \mathbf{u}_i(t) \leq 6.61$, respectively, where $\mathbf{C}_i \in \mathbb{R}^2$ denotes the vector of aggregated battery capacities (kWh) and $\mathbf{1} \in \mathbb{R}^2$ is a vector of ones. The first and second elements of \mathbf{C}_i correspond to the aggregated EV and home battery capacities, respectively, of the prosumers managed by aggregator i . Prosumers have inverters with reactive power import and export limits of 0.33 kVar.

In this framework, each of the $N = 300$ aggregators functions as a decision-maker, approximating the aggregate behavior of its associated prosumers. The utility function for aggregator $i \in \mathcal{N}$ is defined as a quadratic form² $f_i(\mathbf{x}_i(t), \mathbf{u}_i(t)) = -\vartheta_1 \|\mathbf{u}_i(t)\|^2 - \vartheta_{2,t} \|(\mathbf{x}_i(t) - 0.85\mathbf{C}_i) \cdot (1, 0)^\top\|^2 - \vartheta_{3,t} \|(\mathbf{x}_i(t) - 0.85\mathbf{C}_i) \cdot (0, 1)^\top\|^2$ for $t \in \mathcal{T} = \{0, \dots, 47\}$, where $\|\cdot\|$ denotes the Euclidean norm. The terminal utility is given by $\phi_i(\mathbf{x}_i(T)) = -\vartheta_4 \|\mathbf{x}_i(T) - 0.85\mathbf{C}_i\|^2$, with $T = 48$ as the terminal time step. The coefficients ϑ_1 ($10^{-8} \text{¢}/(\text{kW})^2$), $\vartheta_{2,t}$ ($10^{-8} \text{¢}/(\text{kWh})^2$), $\vartheta_{3,t}$ ($10^{-8} \text{¢}/(\text{kWh})^2$), and ϑ_4 ($10^{-8} \text{¢}/(\text{kWh})^2$) serve as regularization weights. For each aggregator i , the power consumed or withdrawn by the aggregated controllable loads (EVs and home battery storage systems) is modeled as $h_i(\mathbf{u}_i(t)) = \mathbf{u}_i(t) \cdot \mathbf{1}$. The feeder nominal voltage is set to $V_0 = 1$ (p.u.). In compliance with the ANSI C84.1 standard, voltage magnitudes must remain within $\pm 5\%$ of the nominal voltage.

B. Numerical Simulations

Considering voltage constraints, the DNSP obtains DOEs according to (3), and sends the obtained $\mathbf{w}_i^*(t)$ to each aggregator i for $i \in \{1, \dots, 300\}$. The DNSP sends the active and reactive power prices, $\lambda^*(t)$ and $\gamma^*(t)$, and DOE limit prices $\beta^*(t)$, which could be obtained solving (6), to each aggregators. Each aggregator i then decides on its electricity consumption and trading to maximize its payoff according to (4). The active and reactive power prices are depicted in Fig. 2, and the DOE limit prices are shown in Fig. 3.

Zero and negative reactive power prices in Fig. 2 correspond to cases where reactive power is in excess in the grid and must be absorbed by inverters. Similarly, zero prices for different elements of DOE limit trading in Fig. 3 indicate that the associated voltage constraints remain within their boundaries, whereas nonzero prices correspond to cases where the respective voltages reach the boundary. The nodal voltages are shown in Fig. 4 and compared with the case without reactive power injection (gray area). As observed, reactive power trading functions as an ancillary service market that improves voltage regulation, with voltages reaching their boundaries less frequently. Moreover, we observed that

²The utility function can take any form, the only requirement is that it is concave.

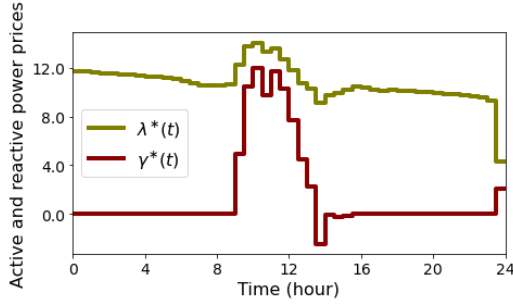


Fig. 2: Active power prices $\lambda^*(t)$ (¢/kWh) and reactive power prices $\gamma^*(t)$ (¢/kVarh), over a 24-hour period (48 time steps of length 0.5 hour).

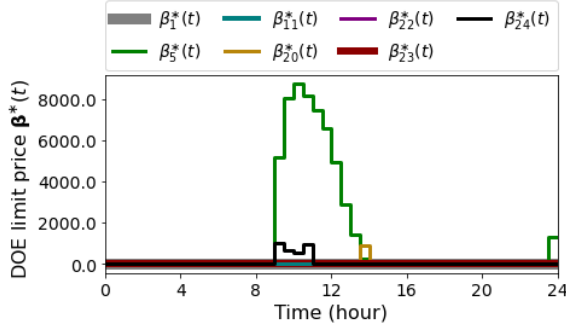


Fig. 3: Some elements of the DOE limit price vector $\beta^*(t)$ (in ¢/(kV)^2) over a 24-hour period (48 time steps of length 0.5 hour). The k -th element of $\beta^*(t)$ is denoted by $\beta_k^*(t)$. The other 17 elements are close to zero and not depicted.

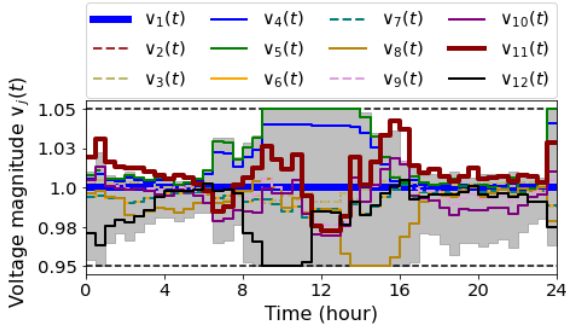


Fig. 4: Nodal voltages $v_j(t)$ (p.u.) for each of the 12 nodes, $j \in \{1, \dots, 12\}$. The gray area indicates the voltage range without reactive power trading across the grid.

reactive power trading increases community profit, as the social welfare of the system rises by 1.6% compared to the case without reactive power trading.

VI. CONCLUSION

We considered a radial distribution feeder operating in island mode to support the blackstart capability of the bulk grid. We designed a peer-to-peer energy market to enable energy trading by prosumers with behind-the-meter rooftop solar backed by battery storage. Moreover, we design the market to incorporate voltage regulation across the feeder

by way of inverter-based resources regulating reactive power flows to and from prosumers. Specifically, we decomposed power flow constraints across the feeder into localized customer-level limits, termed dynamic operating envelopes (DOEs). We showed that our proposed market maximizes social welfare and is equivalent to a standard game. We benchmarked our proposed market using the IEEE 13-node test feeder under binding voltage constraints. Our results demonstrate that reactive power trading functions as an ancillary service market, improving both the community's welfare and the overall voltage profile of the feeder compared to the case without reactive power trading. Future work to consider heterogeneous prosumer utility functions is possible.

REFERENCES

- [1] M. I. Azim et al., "Dynamic operating envelope-enabled P2P trading to maximize financial returns of prosumers," *IEEE Transactions on Smart Grid*, vol. 15, no. 2, pp. 1978–1990, March 2024.
- [2] Y. Meng, J. Qiu, C. Zhang, G. Lei, and J. Zhu, "A Holistic P2P market for active and reactive energy trading in VPPs considering both financial benefits and network constraints," *Applied Energy*, vol. 356, p. 122396, 2024.
- [3] A. Mas-Colell, M. D. Whinston, and J. R. Green, *Microeconomic Theory*, vol. 1. New York: Oxford Univ. Press, 1995.
- [4] K. J. Arrow and G. Debreu, "Existence of equilibrium for a competitive economy," *Econometrica*, vol. 22, no. 3, pp. 265–290, 1954.
- [5] F. Alfaverh, M. Denai, and Y. Sun, "A dynamic peer-to-peer electricity market model for a community microgrid with price-based demand response," *IEEE Transactions on Smart Grid*, vol. 14, no. 5, pp. 3976–3991, Sept. 2023.
- [6] S. Li, J. Lian, A. J. Conejo, and W. Zhang, "Transactive energy systems: The market-based coordination of distributed energy resources," *IEEE Control Syst. Mag.*, vol. 40, no. 4, pp. 26–52, Aug. 2020.
- [7] Z. Salehi, Y. Chen, E. L. Ratnam, I. R. Petersen, and G. Shi, "Competitive equilibrium for dynamic multiagent systems: Social shaping and price trajectories," *IEEE Transactions on Automatic Control*, vol. 69, no. 8, pp. 5184–5199, Aug. 2024.
- [8] Z. Salehi, Y. Chen, E. L. Ratnam, I. R. Petersen, and G. Shi, "Competitive equilibria of multi-agent systems over an infinite horizon," *IFAC-PapersOnLine*, vol. 56, pp. 37–42, 2023.
- [9] G. Lankeshwara, R. Sharma, R. Yan, T. K. Saha, and J. V. Milanović, "Time-varying operating regions of end-users and feeders in low-voltage distribution networks," *IEEE Transactions on Power Systems*, vol. 39, no. 2, pp. 4600–4611, March 2024.
- [10] CutlerMerz. Review of dynamic operating envelopes adoption by DNSPs. Accessed: 2026. [Online]. Available: <https://arena.gov.au/assets/2022/07/review-of-dynamic-operating-envelopes-from-dnsps.pdf>
- [11] M. Mahmoodi, L. Blackhall, S. M. Noori R. A., A. Attarha, B. Weise, and A. Bhardwaj, "DER capacity assessment of active distribution systems using dynamic operating envelopes," *IEEE Transactions on Smart Grid*, vol. 15, no. 2, pp. 1778–1791, 2024.
- [12] L. Li, S. Fan, J. Xiao, Y. Zhang, R. Huang, and G. He, "Energy management strategy for community prosumers aggregated VPP participation in the ancillary services market based on P2P trading," *Applied Energy*, vol. 384, p. 125472, 2025.
- [13] K. Li, L. Wei, J. Fang, X. Ai, S. Cui, M. Zhu, and J. Wen, "Incentive-compatible primary frequency response ancillary service market mechanism for incorporating diverse frequency support resources," *Energy*, vol. 306, 2024.
- [14] D. Aguilar-Dominguez, J. Ejeh, S. F. Brown, and A. D. F. Dunbar, "Exploring the possibility to provide black start services by using vehicle-to-grid," *Energy Rep.*, vol. 8, pp. 74–82, Nov. 2022.
- [15] Y. Zou and Y. Xu, "DER-inverter based reactive power ancillary service for supporting peer-to-peer transactive energy trading in distribution networks," *IEEE Transactions on Power Systems*, vol. 40, no. 1, pp. 753–764, Jan. 2025.
- [16] Z. Jiang and Y. Guo, "Bargaining-based approach for dynamic operating envelope allocation in distribution networks," *IEEE Transactions on Smart Grid*, vol. 16, no. 5, pp. 3588–3600, 2025.

- [17] Z. Salehi, Y. Chen, I. R. Petersen, G. Shi, Duncan S. Callaway, and E. L. Ratnam, "Peer-to-peer energy markets with uniform pricing: A dynamic operating envelope approach," 2025, arXiv:2506.19328.
- [18] I. V. Konnov, "Right-hand side decomposition for variational inequalities," *J. Optim. Theory Appl.*, vol. 160, no. 1, pp. 221–238, 2014.
- [19] D. H. Nguyen, "Optimal Solution Analysis and Decentralized Mechanisms for Peer-to-Peer Energy Markets," *IEEE Transactions on Power Systems*, vol. 36, no. 2, pp. 1470–1481, March 2021. vol. 154, p. 109428, December 2023.
- [20] A. Paudel, M. Khorasany, and H. B. Gooi, "Decentralized local energy trading in microgrids with voltage management," *IEEE Trans. Ind. Informat.*, vol. 17, no. 2, pp. 1111–1121, Feb. 2021.
- [21] N. I. Nimalsiri, E. L. Ratnam, C. P. Mediwaththe, D. B. Smith, and S. K. Halgamuge, "Coordinated charging and discharging control of electric vehicles to manage supply voltages in distribution networks: Assessing the customer benefit," *Appl. Energy*, vol. 291, Jun. 2021, Art. no. 116857.
- [22] Ausgrid. Solar home electricity data. Accessed: 2026. [Online]. Available: <http://linked.data.gov.au/dataset/energy/42966a8f-bc3c-4bde-91d6-91bc5826aa21>
- [23] Battery University. Bu-1003: Electric vehicle (EV). Accessed: 2025. [Online]. Available: https://batteryuniversity.com/article/bu-1003-electric-vehicle-ev#google_vignette
- [24] Y. Wu, S. M. Aziz, and M. H. Haque, "Datasets on probability distributions of arrival and departure times of privately used electric vehicles," *Data in Brief*, vol. 57, p. 110917, 2024. Accessed: 2025. [Online]. Available: <https://data.mendeley.com/datasets/gphwn7sy5n/1>

APPENDIX I PROOF OF THEOREM 1

Let $(\mathbf{U}^*, \mathbf{P}^*, \mathbf{Q}^*, \mathbf{L}^*)$, along with $\lambda^*(t)$, $\gamma^*(t)$, and $\beta^*(t)$ for $t \in \mathcal{T}$, be a competitive equilibrium. Merging optimization problems in (4) for $i \in \mathcal{N}$ implies that $(\mathbf{U}^*, \mathbf{P}^*, \mathbf{Q}^*, \mathbf{L}^*)$ maximizes the social welfare in (6).

The proof of the reverse direction is based on strong duality, which follows from the satisfaction of Slater's condition. Considering the difference equation (1), the state $\mathbf{x}_i(t)$ evolves according to a linear combination of the initial state $\mathbf{x}_i(0)$ and the control input \mathbf{U}_i such that $\mathbf{x}_i(t) = \mathbf{A}_i^t \mathbf{x}_i(0) + \sum_{j=0}^{t-1} \mathbf{A}_i^{t-j-1} \mathbf{B}_i \mathbf{u}_i(j)$ for $t \in \{1, 2, \dots, T\}$, whose substitution into $f_i(\cdot)$ and $\phi_i(\cdot)$ results in $f_i(\mathbf{x}_i(t), \mathbf{u}_i(t)) = \tilde{f}_{i,t}(\mathbf{U}_i)$ and $\phi_i(\mathbf{x}_i(T)) = \tilde{\phi}_i(\mathbf{U}_i)$. The functions $\tilde{f}_{i,t}(\cdot)$ and $\tilde{\phi}_i(\cdot)$ are concave as the composition of a concave function and an affine function. For $i \in \mathcal{N}$, denote $\mathbb{U}_i = \{\mathbf{U}_i | \underline{\mathbf{u}}_i \leq \mathbf{u}_i(t) \leq \bar{\mathbf{u}}_i; \underline{\mathbf{x}}_i \leq \mathbf{x}_i(t) \leq \bar{\mathbf{x}}_i; \underline{p}_i \leq p_i(t) \leq \bar{p}_i; \underline{q}_i \leq q_i(t) \leq \bar{q}_i, \text{ for } t \in \mathcal{T}\}$, which is a polyhedral set. For any $(\mathbf{U}, \mathbf{P}, \mathbf{Q}, \mathbf{L})$ such that $\mathbf{U}_i \in \mathbb{U}_i$, the Lagrangian function of (6) is defined as

$$\begin{aligned} \mathcal{L}(\mathbf{U}, \mathbf{P}, \mathbf{Q}, \mathbf{L}, \alpha, \vartheta, \delta, \Psi, \Pi) = & \\ & - \sum_{i=1}^N \left(\sum_{t=0}^{T-1} \tilde{f}_{i,t}(\mathbf{U}_i) + \tilde{\phi}_i(\mathbf{U}_i) \right) + \sum_{t=0}^{T-1} \alpha(t) \left(- \sum_{i=1}^N p_i(t) \right) \\ & + \sum_{t=0}^{T-1} \vartheta(t) \left(- \sum_{i=1}^N q_i(t) \right) + \sum_{t=0}^{T-1} \delta(t) \cdot \left(- \sum_{i=1}^N \mathbf{l}_i(t) \right) \\ & + \sum_{t=0}^{T-1} \sum_{i=1}^N \psi_i(t) \left(p_i(t) + h_i(\mathbf{u}_i(t)) - a_i(t) \right), \\ & + \sum_{t=0}^{T-1} \sum_{i=1}^N \pi_i(t) \cdot \left(\mathbf{l}_i(t) + \mathbf{g}_i(p_i(t)) - \mathbf{w}_i^*(t) \right), \end{aligned} \quad (9)$$

where $\psi_i(t) \geq 0$, $\pi_i(t) \geq 0$, $\alpha = (\alpha(0), \dots, \alpha(T-1))^\top$, $\vartheta = (\vartheta(0), \dots, \vartheta(T-1))^\top$, $\delta =$

$(\delta^\top(0), \dots, \delta^\top(T-1))^\top$, $\Psi_i = (\psi_i(0), \dots, \psi_i(T-1))^\top$, and $\Psi = (\Psi_1^\top, \dots, \Psi_N^\top)^\top$. We define Π_i and Π in a similar way. The Lagrangian (9) is separable such that

$$\begin{aligned} \mathcal{L}(\mathbf{U}, \mathbf{P}, \mathbf{Q}, \mathbf{L}, \alpha, \vartheta, \delta, \Psi, \Pi) & \\ = \sum_{i=1}^N \mathcal{L}_i(\mathbf{U}_i, \mathbf{p}_i, \mathbf{q}_i, \mathbf{L}_i, \alpha, \vartheta, \delta, \Psi_i, \Pi_i), & \quad (10) \end{aligned}$$

where

$$\begin{aligned} \mathcal{L}_i(\mathbf{U}_i, \mathbf{p}_i, \mathbf{q}_i, \mathbf{L}_i, \alpha, \vartheta, \delta, \Psi_i, \Pi_i) = & \\ & - \sum_{t=0}^{T-1} \left(\tilde{f}_{i,t}(\mathbf{U}_i) \right. \\ & \left. + \alpha(t)p_i(t) + \vartheta(t)q_i(t) + \delta(t) \cdot \mathbf{l}_i(t) \right) - \tilde{\phi}_i(\mathbf{U}_i) \\ & + \sum_{t=0}^{T-1} \psi_i(t) \left(p_i(t) + h_i(\mathbf{u}_i(t)) - a_i(t) \right) \\ & + \sum_{t=0}^{T-1} \pi_i(t) \cdot \left(\mathbf{l}_i(t) + \mathbf{g}_i(p_i(t)) - \mathbf{w}_i^*(t) \right). \end{aligned}$$

Let $(\mathbf{U}^*, \mathbf{P}^*, \mathbf{Q}^*, \mathbf{L}^*)$ be an optimal primal solution to (6), and $(-\alpha^*, -\vartheta^*, -\delta^*, \Psi^*, \Pi^*)$ be an optimal dual solution. Given that Slater's condition is satisfied, strong duality implies

$$\begin{aligned} (\mathbf{U}^*, \mathbf{P}^*, \mathbf{Q}^*, \mathbf{L}^*) & \\ \in \arg \min_{\mathbf{U}, \mathbf{P}, \mathbf{Q}, \mathbf{L}} \mathcal{L}(\mathbf{U}, \mathbf{P}, \mathbf{Q}, \mathbf{L}, \alpha^*, \vartheta^*, \delta^*, \Psi^*, \Pi^*), & \quad (11) \end{aligned}$$

for $\mathbf{U}_i \in \mathbb{U}_i$. Considering (10) and (11), there holds

$$\begin{aligned} (\mathbf{U}_i^*, \mathbf{p}_i^*, \mathbf{q}_i^*, \mathbf{L}_i^*) & \\ \in \arg \min_{\mathbf{U}_i, \mathbf{p}_i, \mathbf{q}_i, \mathbf{L}_i} \mathcal{L}_i(\mathbf{U}_i, \mathbf{p}_i, \mathbf{q}_i, \mathbf{L}_i, \alpha^*, \vartheta^*, \delta^*, \Psi_i^*, \Pi_i^*), & \quad (12) \end{aligned}$$

for $\mathbf{U}_i \in \mathbb{U}_i$. In addition, strong duality implies

$$\begin{aligned} (\alpha^*, \vartheta^*, \delta^*, \Psi^*, \Pi^*) & \\ \in \arg \max_{\alpha, \vartheta, \delta, \Psi, \Pi} \min_{\mathbf{U}, \mathbf{P}, \mathbf{Q}, \mathbf{L}} \mathcal{L}(\mathbf{U}, \mathbf{P}, \mathbf{Q}, \mathbf{L}, \alpha, \vartheta, \delta, \Psi, \Pi) & \\ = \arg \max_{\alpha, \vartheta, \delta, \Psi, \Pi} \min_{\mathbf{U}, \mathbf{P}, \mathbf{Q}, \mathbf{L}} \sum_{i=1}^N \mathcal{L}_i(\mathbf{U}_i, \mathbf{p}_i, \mathbf{q}_i, \mathbf{L}_i, \alpha, \vartheta, \delta, \Psi_i, \Pi_i), & \end{aligned}$$

and, therefore, $(\Psi_i^*, \Pi_i^*) \in \arg \max_{\Psi_i, \Pi_i} \min_{\mathbf{U}_i, \mathbf{p}_i, \mathbf{q}_i, \mathbf{L}_i} \mathcal{L}_i(\mathbf{U}_i, \mathbf{p}_i, \mathbf{q}_i, \mathbf{L}_i, \alpha^*, \vartheta^*, \delta^*, \Psi_i, \Pi_i)$, where the primal and dual variables are in their respective domains. Considering $\lambda^*(t) = \alpha^*(t)$, $\gamma^*(t) = \vartheta^*(t)$, and $\beta^*(t) = \delta^*(t)$ for $t \in \mathcal{T}$, the function $\mathcal{L}_i(\mathbf{U}_i, \mathbf{p}_i, \mathbf{q}_i, \mathbf{L}_i, \alpha^*, \vartheta^*, \delta^*, \Psi_i, \Pi_i)$ is the Lagrangian of (4). Therefore, (Ψ_i^*, Π_i^*) is an optimal dual solution of (4). Given that Slater's condition is satisfied, strong duality implies that according to (12), $(\mathbf{U}_i^*, \mathbf{P}_i^*, \mathbf{Q}_i^*, \mathbf{L}_i^*)$ is an optimal primal solution of (4) which satisfies (5). Consequently, $(\mathbf{U}^*, \mathbf{P}^*, \mathbf{Q}^*, \mathbf{L}^*)$, along with $\lambda^*(t) = \alpha^*(t)$, $\gamma^*(t) = \vartheta^*(t)$, and $\beta^*(t) = \delta^*(t)$ for $t \in \mathcal{T}$, forms a competitive equilibrium.